THE JOURNAL OF PHYSICAL CHEMISTRY C

Article

Cite This: J. Phys. Chem. C 2019, 123, 11823−11832

pubs.acs.org/JPCC

BT-2-BOX: An Assembly toward Multimodal and Multilevel Molecular System Simple as a Breeze

Youssef Aidibi,[†] Clément Guerrin,[‡] Olivier Alévêque,[†] Philippe Leriche,[†] Stéphanie Delbaere,[‡] and Lionel Sanguinet*[,†]

[†]MOLTECH-Anjou, UMR 6200, CNRS, Université Angers, 2 bd Lavoisier, 49045 Angers Cedex, France

[‡]Université Lille, CNRS, UMR 8516—LASIR, F-59000 Lille, France

Supporting Information

ABSTRACT: The design of multistate/multifunctional molecular systems arouses a lot of interest. Such compounds are able to commutate between two metastable states by the application of an external stimulation such as light, heat, protons, or electrons. In this context, we are interested in molecular switches based on indolino-oxazolidine (BOX) which is a relatively less-known sub-class of multimodal addressable units. Their particularity consists of the possibility to induce the opening/closing of the oxazolidine ring by using indifferently light, electrochemical, or acido-basic stimulation. Up to now, most of the reported systems based on BOX have allowed to modulate a molecular property but only between two discrete levels which can only be extended by their association with other classical switchable unit such as a dithienylethene unit. For this reason, we report here our effort to enhance the number of metastable states by simply connecting two identical BOX units by a bithiophene (BT) linker. The resulting system's ability to switch between the three possible metastable states was investigated. Irrespective of the nature of the stimulation, full commutation of the system could be reached, but our work mainly revealed that the opening of both oxazolidine rings occurs in a stepwise manner. If this unreported selectivity upon a unique stimulus with two identical switchable units is observed irrespective of the stimulation, it must be pointed out that its efficiency depends on the nature of the latter. The direct stimulation with acid or light leads to the coexistence of the three different states of the system over a broad stimulation period. On the contrary, the indirect stimulation of BOX via an electromediated process due to the electroactivity of BT enhances the selective addressability between both identical BOX units.

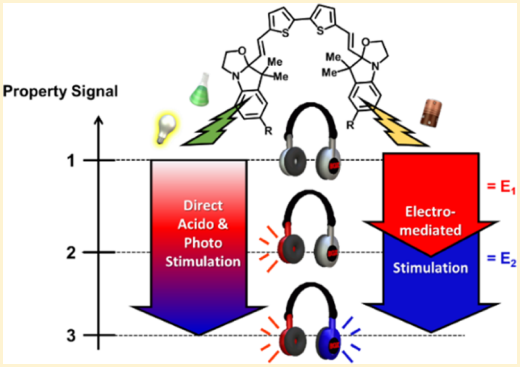

INTRODUCTION

Nowadays, big data storage is mainly assured by magnetic and optical systems. Both technologies lay down on the same principle and can be roughly resumed as the possibility to commutate molecular systems or domains under an external stimulation, such as magnetic field or light irradiation between two metastable states exhibiting different physico-chemical properties. In order to increase the storage capacity, a multiplexing recording method represents a promising approach which leads to the development of multilayer recording media containing different dyes presenting orthogonal stimulation responsivenesses.[1−3] This multiplexing concept can be extended at the molecular level, by the integration of several switchable or multiaddressable functions into a single molecule connected covalently[4,5] or via a supramolecular assembly process.[6] Indeed, the combination of n switches shapes a multiswitch system which can exhibit up to 2^n various states and brings new perspectives for the design of molecular-scale high-density optical memory or multinary logic devices.[7−9]

In this context, numerous molecular systems combining different types of switchable moieties have been reported.[10−12] If the development of photo- and redox-active materials is particularly attractive for applications in molecular memories or logic gates,[13−15] their selective addressability is still quite challenging when several switching units of the same type are present especially when the stimulus is light. For example, numerous systems incorporating several diarylethene (DAE) units, undoubtedly the most studied photoswitch family,[16−27] exhibit restricted photochromic performances. In most cases, it is not possible to address specifically one of those and even worse, the photocyclization of one DAE unit impedes the photoreactivity of the remaining ones and, as consequence, the fully closed forms of these multichromophoric systems can hardly be obtained.[28]

In order to circumvent these selectivity and reactivity issues, the use of multimodal switching molecules that can be interconverted from one state to another by using indifferently several kinds of stimulation (i.e., light, redox potential, and magnetic field) represents a promising approach. Beside the

Received: January 18, 2019
Revised: April 1, 2019
Published: April 16, 2019

DOI: 10.1021/acs.jpcc.9b00546
J. Phys. Chem. C 2019, 123, 11823−11832

classical DAE, indolino-oxazolidine (referenced later as BOX) derivatives are a relatively confidential sub-class of multimodal addressable units known to display photo- and acido-chromic performances.[29−32] Moreover, we have recently reported the possibility to induce the opening and closure of the oxazolidine ring under an electrochemical stimulation. It is important to notice that the electroinduced opening of the oxazolidine can result from two different processes depending on the substitution pattern of the BOX such as the nature of the π-conjugated system associated with position 2. Indeed, both systems acting independently under the closed form, the first oxidation of the system could then occur either on the BOX moiety (direct electrostimulation)[33] or on the associated aromatic system (mediated electrostimulation)[34] depending on the relative position of their oxidation potential. In this context, we report here on the functionalization of a bithiophene (BT) moiety as a well-known redox probe[35] by two identical BOX units and on the studies of their commutation properties under the application of an external stimulation (proton, photon, and electron).

EXPERIMENTAL SECTION

Synthesis. Commercially available (Aldrich, Alfa Aesar, and abcr) chemicals such as BT were used as received. The 2,2′-bithiophene-5,5′-dicarbaldehyde was prepared according to an already reported procedure,[36] as well as the different substituted indolino-oxazolidines.[37,38] All compounds were purified by flash chromatography using technical grade silica gel (Fluka, 60 Å pore size, 230−400 Å mesh).

General Procedure. For all functionalizations of the BT by the BOX unit, the following experimental procedure was used. A mixture of 2,2′-bithiophene-5,5′-dicarbaldehyde (1.35 mmol) and corresponding indolino-oxazolidine (2.7 mmol) was dissolved in little amount of acetonitrile (ACN). Technical grade silica (1.35 g) was put in suspension, and the solvent was removed under reduced pressure. The resulting reaction mixture was heated under stirring at 100 °C during 10 min. After cool down to room temperature, the crude material was directly purified by flash chromatography (dichloromethane/methanol, 98/2).

Compound **1**, *BOX-H*. Product was isolated as a yellow solid (496 mg, 62%). mp: 170−173 °C. ^{1}H NMR (300 MHz, $CDCl_3$): δ (ppm) 7.17 (td, J = 7.7, 1.3 Hz, 1H), 7.09 (d, J = 7.4 Hz, 1H), 7.05 (d, J = 3.7 Hz, 1H), 6.98−6.91 (m, 3H), 6.80 (d, J = 7.7 Hz, 1H), 6.11 (d, J = 15.6 Hz, 1H), 3.83−3.42 (m, 4H), 1.45 (s, 3H), 1.18 (s, 3H).·^{13}C NMR (75 MHz): δ (ppm) 20.37, 28.44, 48.14, 50.17, 63.67, 109.65, 112.07, 121.80, 122.43, 124.05, 125.45, 126.07, 127.51, 127.67, 136.43, 139.70, 140.83, 150.45. IR ν (cm^{-1}): 2969, 1739, 1365, 1216, 746 cm^{-1}. HRMS (FAB+) m/z: calcd for $C_{36}H_{36}N_2O_2S_2$, 592.22 $[M + H]^+$; found, 593.2299. Anal. Calcd (%) for $C_{36}H_{36}N_2O_2S_2$: C, 72.94; H, 6.12; S, 10.82; N, 4.73. Found: C, 72.79; H, 6.35; S, 10.41; N, 4.58.

Compound **2**, *BOX-Me*. Product was isolated as a yellow solid (460 mg, 55%). mp: 232−235 °C. ^{1}H NMR (300 MHz, $CDCl_3$): δ (ppm) 7.04 (d, J = 3.7 Hz, 1H), 7.00−6.87 (m, 4H), 6.70 (d, J = 7.9 Hz, 1H), 6.10 (d, J = 15.3 Hz, 1H), 3.82−3.40 (m, 4H), 2.31 (s, 3H), 1.42 (s, 3H), 1.16 (s, 3H). ^{13}C NMR (75 MHz): δ (ppm) 20.32, 21.04, 28.45, 48.14, 50.30, 63.65, 109.94, 111.82, 123.50, 124.03, 125.36, 126.22, 127.41, 128.12, 131.21, 136.46, 139.78, 140.89, 148.10. IR ν (cm^{-1}): 2969, 1739, 1363, 1215, 808 cm^{-1}. HRMS (FAB+) m/z: calcd for $C_{38}H_{40}N_2O_2S_2$, 620.25 $[M + H]^+$; found, 621.2623. Anal. Calcd (%) for $C_{38}H_{40}N_2O_2S_2$: C, 73.51; H, 6.49; S, 10.33; N, 4.51. Found: C, 72.45; H, 6.43; S, 10.25; N, 4.45.

Compound **3**, *BOX-F*. Product was isolated as a yellow solid (568 mg, 67%). mp: 200−204 °C. ^{1}H NMR (300 MHz, $CDCl_3$): δ (ppm) 7.05 (d, J = 3.8 Hz, 1H), 6.98−6.90 (m, 2H), 6.85 (td, J = 8.8, 2.6 Hz, 1H), 6.79 (dd, J = 8.3, 2.5 Hz, 1H), 6.70 (dd, J = 8.5, 4.3 Hz, 1H), 6.08 (d, J = 15.7 Hz, 1H), 3.84−3.39 (m, 4H), 1.42 (s, 3H), 1.17 (s, 3H). ^{13}C NMR (75 MHz): δ (ppm) 20.20, 28.26, 48.32, 50.50, 63.69, 109.75, 110.06, 110.16, 112.42, 112.53, 113.66, 113.97, 124.09, 125.64, 125.70, 127.61, 136.54, 140.72, 141.43, 141.53, 146.28, 157.36, 160.52. ^{19}F NMR (283 MHz, $CDCl_3$): δ −122.67. IR ν (cm^{-1}): 2968, 1739, 1480, 1365, 1204, 807 cm^{-1}. HRMS (FAB+) m/z: calcd for $C_{38}H_{40}N_2O_2S_2$, 628.20 $[M + H]^+$; found, 629.2109. Anal. Calcd (%) for $C_{36}H_{36}N_2O_2S_2$: C, 68.76; H, 5.45; S, 10.2; N, 4.46. Found: C, 68.86; H, 5.49; S, 9.72; N, 4.25.

NMR Experiments. NMR spectra were recorded on 500 or 300 spectrometers (^{1}H, 500 MHz, ^{13}C, 125 MHz, or ^{1}H, 300 MHz, ^{13}C, 75 MHz) equipped with triple resonance inverse or Quattro nucleus probes, using standard sequences. Data sets were processed using Bruker TopSpin 3.2 software. Samples were dissolved in acetonitrile-d^3 in NMR tubes. Irradiation with 254 nm light was achieved in rotating quartz NMR tubes (5 mm) at 295 K with a Bioblock Scientific VL-6LC lamp (12 W).

Cyclic Voltammetry. ACN [high-performance liquid chromatography (HPLC) grade] and tetra-*n*-butylammonium hexafluorophosphate (TBAP, electrochemical grade, Fluka, recrystallized from ethanol) were, respectively, used as a solvent and electrolyte. Cyclic voltammetry (CV) was performed in a three-electrode cell equipped with a platinum millielectrode, a platinum wire counter-electrode, and a silver wire used as a quasi-reference electrode. The electrochemical experiments were carried out under a dry and oxygen-free atmosphere (H_2O < 1 ppm, O_2 < 1 ppm) in CH_2Cl_2 with TBAP (0.1 M) as the support electrolyte. The voltammograms were recorded on a potentiostat/galvanostat (BioLogic—SP150) driven by the EC-Lab software with positive feedback compensation. On the basis of repetitive measurements, absolute errors on potentials were estimated to be ≈±5 mV. All of the potential reported were calibrated versus ferrocene/ferrocenium oxidation potential (+0.405 V vs saturated calomel electrode or +0.425 V vs Ag/AgCl).

Time-Resolved Spectroelectrochemistry. Time-resolved spectroelectrochemistry was performed using the already described home self-made cell.[39] A distance of 25−200 μm between the surface of the electrode and the optical window was typically used in our experiments. Electrochemical measurements were carried out using a platinum wire counter electrode and a silver wire as a quasi-reference electrode with a BioLogic SP-150 potentiostat driven by the EC-Lab software including Ohmic drop compensation. Experiments were recorded in dry HPLC-grade ACN with tetrabutylammonium hexafluorophosphate (Bu_4NPF_6, electrochemical grade, Fluka) as a supporting electrolyte. All solutions were prepared and transferred into the spectroelectrochemical cell in a glovebox containing dry, oxygen-free (<1 ppm) argon, at room temperature. Spectrophotometric measurements were carried out with a home-made bench composed of different Princeton Instruments modules (light sources, fibers, monochromators, spectroscopy camera, and software). To start the two

DOI: 10.1021/acs.jpcc.9b00546
J. Phys. Chem. C 2019, 123, 11823−11832

Scheme 1. Elaboration of the Three Different Multichromophoric Systems Based on the BT Central Core

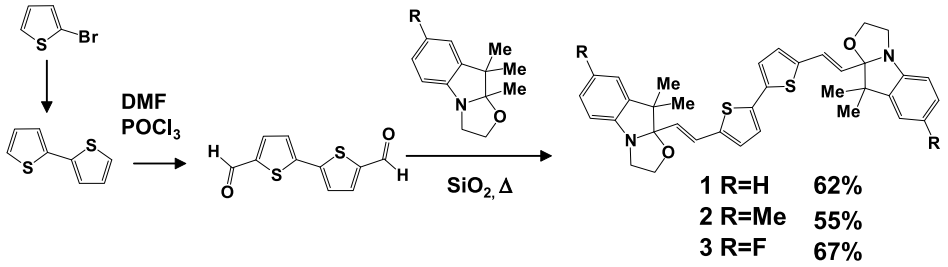

experiments at the same time, the two benches are synchronized with transistor-transistor logic signals.

RESULTS AND DISCUSSION

Synthesis. The connection of several switchable units together is not something straightforward and requires generally a lot of synthetic efforts. The use of BOX as a multimodal switching unit facilitates greatly the preparation of multichromophoric systems. Indeed, the functionalization of a π-conjugated system by a BOX unit could be simply resumed to a condensation between an aromatic aldehyde and the trimethylindolino-oxazolidine. Most of the time, this reaction is carried out in boiling ethanol and requires extended reaction time as long as several days. For this reason, we have recently reported a silica-mediated synthesis[37] allowing a drastical reduction of the reaction time from several days to few minutes and assuring good selectivity when several aldehyde functions are present on the aromatic partner. Beside it, the preparation of 2,2′-bithiophene-5,5′ dicarboxaldehyde is largely documented and its reactivity such as in Knoevenagel condensation is also well known.[36] Starting from this, the preparation of the targeted multichromophoric systems using different substituted indolino-oxazolidines did not meet particular difficulties and is summarized below (Scheme 1).

The three compounds differ from the substituent nature in position 5 of the indoline heterocycle, which were chosen to facilitate the investigation of the commutation ability. Indeed, the comparison of their electrochemical behavior could lead to determine the localization of the first oxidation process. When the oxidation is mainly localized on the BOX units, different electrochemical processes are observed as a function of the substituent in position 5. A nude derivative (R = H) is known to undergo dimerization, whereas a methyl group avoids it and promotes the oxazolidine ring opening, while, at the opposite, a fluorine atom stabilizes the corresponding radical cation.[33] Moreover, the presence of a fluorine atom (compound **3**) is also an elegant manner to quantify the different metastable states thanks to ^{19}F NMR spectroscopy (vide infra).

Acidochromic Properties. Under their closed forms, all compounds present almost identical UV−visible spectra with a maximum absorption wavelength of 378−379 nm, showing only a slight effect of the substituent on the epsilon value (Table 1). Associated with the slight peak structuration, this maximal absorption band is assigned to the central BT moiety in agreement with the reported optical properties of various 5,5′-disubstitued-2,2-bithiophene derivatives.[40] Moreover, the sp^3 hybridization of the carbons linking the BOX unit to the central vinyl-bithiophene node breaks the conjugation and leads to a central and two lateral independent π-conjugated systems which explains the poor effect of the substituent on the absorption maxima wavelength of the three different systems

Table 1. UV−Visible Spectra of Compounds 1, 2, and 3 under Their CC Form in ACN Solution and the Evolution of the Maxima Absorption Wavelength (in nm) under Their Different Metastable States

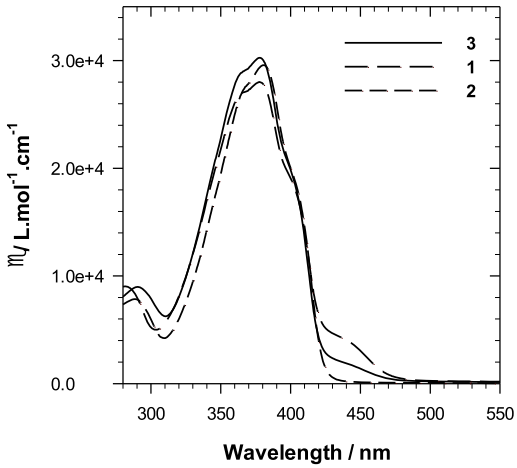

compound λ_{max}	CC	OC	OO
1	378	529	546
2	379	533	561
3	378	538	552

under their **CC** (closed−closed) form. In all cases, the addition of acid (aq HCl) to the solution induces a deep pink coloration associated with the appearance of an intense broad band in the visible 450−600 nm range. More importantly, the initial state of the solution is restored instantaneously by addition of some base such as NEt_3.

The acidic pH changes lead at the end to the opening of both oxazolidine rings, resulting in the generation of corresponding indoleninium acting as strong withdrawing groups, as well as the extension of the π conjugation on the whole molecule. Nevertheless, the presence of two switching units lets presume the possibility to progressively generate 3 different states under acidic stimulation, referenced later in the text as **CC**, **OC**, and **OO**, depending on closed (C) or open (O) status of each BOX units (Scheme 2).

Up to now, the only reported molecular system incorporating several BOX units was constituted on two of them separated by a DAE moiety. This complex molecular system did not allow addressing selectively each BOX unit under acidic stimulation whatever the open/closed status of the DAE.[41] These results were explained by the almost orthogonality of the BOX units with regard to their olefinic substituent which leads to consider no interaction through bonds between them.[41]

DOI: 10.1021/acs.jpcc.9b00546
J. Phys. Chem. C 2019, 123, 11823−11832

Scheme 2. Representation of the 3 Different States of the Molecular System: CC, OC, and OO, Depending on Closed (C) or Open (O) Status of BOX Units

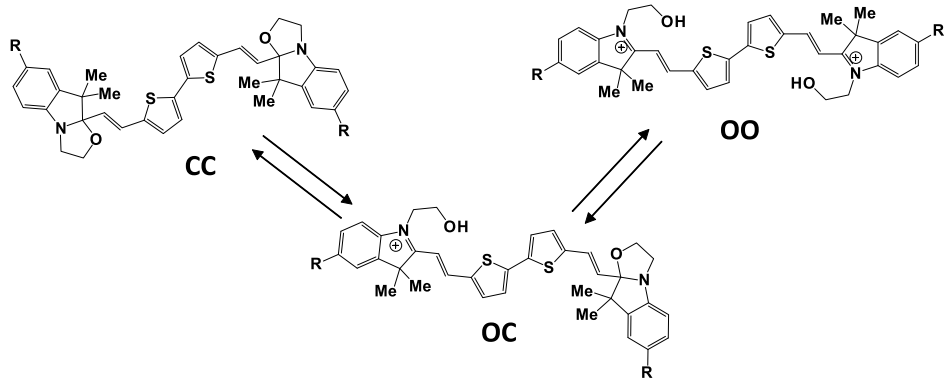

In contrary, in the case of compounds **1**−**3**, the observation of an irregular evolution of the UV−visible spectra along the titration with acid aliquots could translate a stepwise opening of the BOX units. Such as presented in Figure 1 for compound **1** as example, up to 1 equiv, the UV spectra reveal the appearance of a unique band centered at 529 nm as well as a strong decrease of the band intensity at 378 nm. More importantly, below 1 equiv, the presence of two isosbestic points at 321 and 417 nm indicates that only two species are in equilibrium and then deduced to be **CC** and **OC**. To induce the ring opening in the second BOX unit, the added quantity of HCl is pushed further than 1 equiv. It leads to an enhancement of the solution coloration with the complete disappearance of the band at 378 nm. In addition, a bathochromic shift of the main absorption band from 529 to 546 nm is observed with the concomitant appearance of two small higher-energy absorption bands at 311 and 431 nm, respectively. More importantly, this increment of the acid quantity did not allow maintaining the observation of the previous isosbestic points at 321 and 417 nm which are replaced by a unique one at 326 nm possibly associated with equilibrium between **OC** and **OO** forms. As a consequence, this experiment suggests the commutation of the connected BOX units in a stepwise manner.

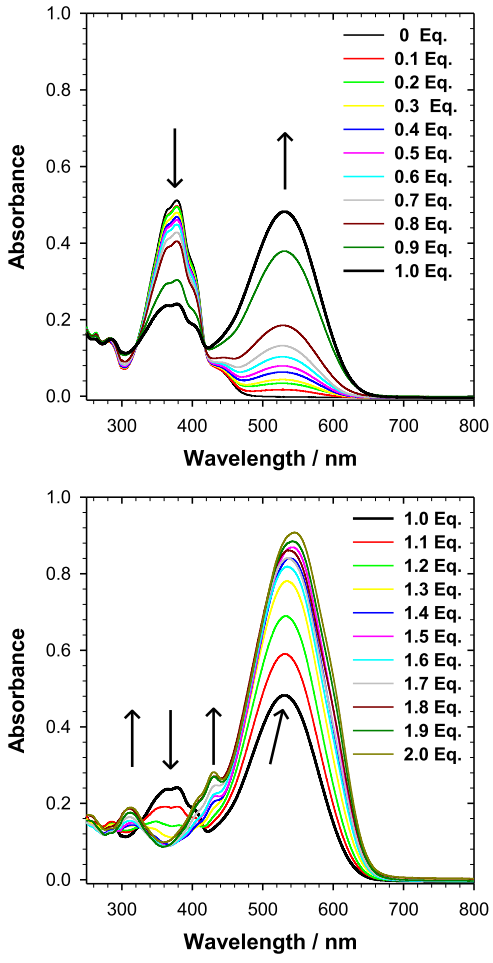

Figure 1. UV−visible spectrum changes of a solution of **BOX-H** in ACN (0.021 mM) upon addition of HCl (aqueous) aliquots.

If the UV−visible spectroscopy appears as the most convenient technique to monitor the commutation of elaborated systems under stimulation, NMR spectroscopy has been here used to unambiguously confirm the stepwise commutation of both BOX units. Although the identification of each metastable states (**CC**, **OC**, and **OO** forms) was confirmed by ^{1}H NMR (see the Supporting Information), the introduction of the fluorine atom in position 5 (compound **3**) facilitates their quantification. As expected, the ^{19}F NMR spectrum of compound **3** under its initial state (**CC**) exhibits only one signal at −124.73 ppm in agreement with the existence of an element of symmetry between both BOX units. As soon as the addition of HCl aliquots starts, the appearance of two new peaks is observed at −124.60 and −112.29 ppm (Figure 2) which can be reasonably assigned to the **OC** form. Indeed, the breaking of the molecular symmetry due to the commutation of only one BOX unit leads to two low-field shifted peaks in comparison with the **CC** form and exhibiting a similar integration.

As we can see in Figure 2, the distribution between the three different states is not statistically driven and the stepwise opening of both BOX units is clearly confirmed. This behavior seems translating a difference of pK_a between both protonation processes. This assignment was confirmed by the clear appearance of only one new signal at −111.84 ppm when the amount of HCl was increased beyond 0.8 equiv in agreement with the re-establishment of a molecular symmetry with the opening of the second BOX unit. In this context, the integration of the different peaks can be used to determine the relative proportion of the three different states of the molecule as a function of the added amount of acid (Figure 2).

DOI: 10.1021/acs.jpcc.9b00546
J. Phys. Chem. C 2019, 123, 11823−11832

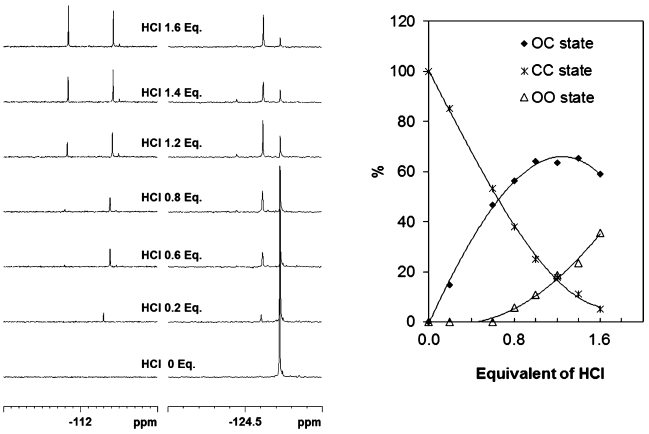

Figure 2. ^{19}F NMR spectra (left) and deduced quantification (right) of the 3 different states in a solution of **BOX-F** in ACN (2.27 mM) upon addition of HCl aliquots.

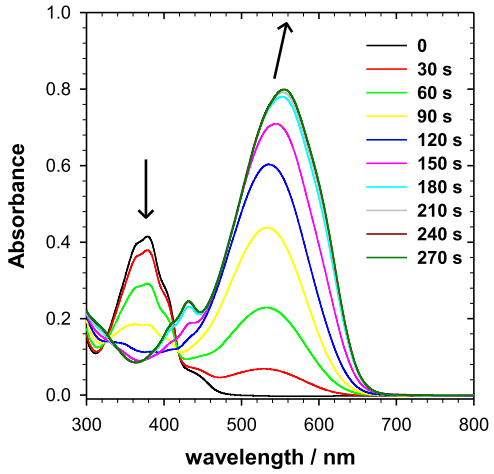

Figure 3. UV−visible spectrum changes of a solution of **1** in ACN/PhCl (90/10; 0.016 mM) upon UV light irradiation (254 nm).

However, it is important to notice that the limited solubility of compound **3** under its **OO** form in ACN induces an experimental limitation to this quantification because of its partial precipitation after 1.8 equiv of HCl. Considering each BOX unit being independent under their closed form due to the sp^3 hybridization of the carbon 2, such difference could be explained by a variation of the donor ability of the associated conjugated system which is involved in the stabilization of the corresponding open form. In fact, the first opening of an oxazolidine ring induces the generation of the corresponding indoleninium group which acts as a strong electron-withdrawing group and decreases the donor character of the BT moiety. As a consequence, the BT moiety is not able to stabilize the dicationic species by internal charge transfer as efficiently as the monocationic one. In these conditions, the opening of the second BOX appears more difficult than that of the first one.

In addition, it can be noticed that the presence of **CC** form is still detected after 1.6 equiv of acid leading to an unsuitable coexistence of the three different forms over a large period of stimulation incompatible with a sharp modulation of molecular properties over three discrete levels. Knowing the multimodal commutation properties of the BOX, the other kind of stimuli was explored in order to improve the addressability selectivity between both connected BOX units.[29−32]

Photochromic Properties. Among the different stimuli able to induce the BOX oxazolidine ring opening reported so far, light irradiation stays one of the most used because of its promising potential applications.[32] On the basis of our previous works on simple dyad BT-BOX,[34] ACN solutions of **1**, **2**, and **3** have been irradiated with 254 nm light in the presence of chlorobenzene (10%) as a photosensitizer. As expected, the UV irradiation leads quickly to the strong coloration of the solution, reaching a photostationary state after 4 min. The evolution of the UV−visible absorption spectra as a function of the irradiation time lets clearly appear two stages such as an example for compound **1** presented in Figure 3. Below 2 min of irradiation duration, the appearance of an absorption band centered at 529 nm is concomitant with the reduction of the absorption at 378 nm as well as the presence of two isosbestic points at 321 and 417 nm. Upon longer irradiation time (t > 120 s), the visible absorption band continues to increase but is also bathochromically shifted and associated with the appearance of two weak bands at higher energy. More importantly, both isosbestic points are not anymore clearly defined, suggesting that more than two different species are in equilibrium at this stage. As mentioned in our previous work, water traces contained in ACN induce the protonation and solvation of the photogenerated form leading to a protonated open form thus preventing a quantitative ring closure under visible irradiation.[34] However, the addition of base allows quantitatively, once again, the restoration of the initial **CC** state of the system. In fact, if the first opening of the BOX seems to occur at first place, several photochemical processes can be suggested after that such as the second oxazolidine ring opening, the cis/trans isomerization of one ethylenic junction,[42] photooxidation process,.[43].. However, the overlapping of the UV−visible spectra obtained by either irradiation or acidic titration is noticed, then translating that both stimuli lead to the same commutations, and then, confirming the multimodal switching abilities of these molecular systems. As the molecular structure of each possible state presents a unique spectral signature, ^{1}H NMR has been used to confirm the photochemical response of compound **3** in the same conditions of solvent (90% ACN-d_3 + 10% of chlorobenzene-d_5) and irradiation (254 nm).

Noteworthy, in order to clearly identify the nature of photoproducts, higher concentrations are required for NMR technique. The closed-ring of the BOX is evidenced by two patterns of unresolved multiplets for methylene protons of N−CH_2−CH_2−O between 3.3 and 3.9 ppm, whereas two well-resolved triplets between 4.0 and 5.0 ppm characterize the ring opening (see Figures S12−S14). The trans configuration of the ethylenic protons is confirmed by vicinal coupling constants of 16−17 Hz for both doublets at 6.2 and 7.1 ppm. In the case of compound **3**, upon successive periods of irradiation, the decrease of signals of initial **CC** state is observed along with the gradual appearance of new resonances. More particularly, **CC** (Scheme 2) presents a relatively simple spectrum because of the symmetry of the system (see Figure S15), when a higher number of resonances is detected for the new photoproduct, suggesting a dissymmetrical structure. Really, the **OC** state (Scheme 2) is identified by two well-resolved triplets at 4.0 and 4.6 ppm and a pattern between 3.5 and 4.0 for the two methylene groups in open and closed BOX, respectively, associated with four doublets at 6.2 and 7.1 ppm (closed BOX side) and 7.6 and 8.4 ppm (open BOX side) for the ethylenic

DOI: 10.1021/acs.jpcc.9b00546
J. Phys. Chem. C 2019, 123, 11823−11832

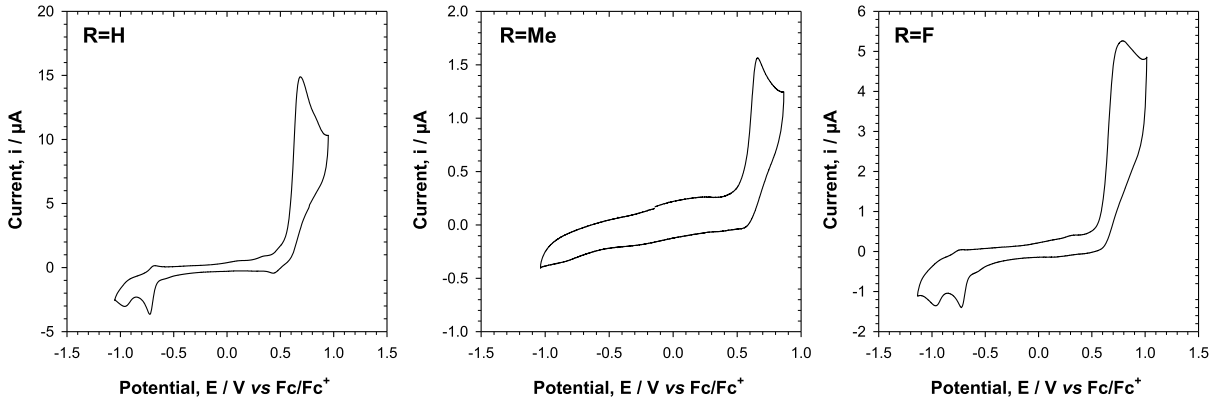

Figure 4. CV of compounds **1**, **2**, and **3** in ACN (1.12; 0.53 and 0.68 mM) with TBAP as an electrolyte (0.1 M) on the Pt working electrode at 100 $mV{\cdot}s^{-1}$.

protons. When irradiation time is increased (see Figure S15), these signals disappear and, finally, a simple spectrum is observed with more particularly, two triplets at 4.1 and 4.7 ppm and two doublets at 7.55 and 8.45 ppm, thus proving the opening of the two BOX entities in a symmetrical structure, namely, **OO** (Scheme 1). Consequently, UV light irradiation leads to the stepwise opening of BOX units, but with a relatively low efficiency and selectivity. Indeed, after 10 min of illumination, only 20% of **OC** is detected. Increasing the illumination time up to 40 min not only allows to produce 50% of **OC** but also with 10% of **OO**. Finally, the total conversion of **CC** and **OC** is obtained after 90 min of irradiation. Such long response is easily explained by the concentration of the NMR samples which is higher than concentrations used for UV−visible spectroscopy, then requiring longer time of irradiation. However, these experiments clearly demonstrated that light irradiation is not the most suitable stimulus to get efficient and selective commutations between **CC**, **OC**, and **OO** forms. Thus, we looked for another stimulus to reach this objective.

Electrochromic Properties. As mentioned above, the BOX opening can also be induced by an electromediated process when this unit is associated with an electroactive moiety such as BT.[34,44] At the opposite of acid and light stimuli where the processes are mainly localized on the BOX units, we can assume that they are not directly stimulated in these conditions but via the BT core. Moreover, such electrochemical process should lead to a better selectivity of commutations than other kinds of stimulation. Indeed, after the first electrochemical opening, the obtained **OC** compounds exhibit a central BT conjugated with the electron-withdrawing open BOX what decreases the global donor ability of the system and then complicates the second opening. Consequently, the second oxazolidine ring opening may appear more difficult, leading to an increased discrimination between **OC** and **OO** states of the molecular system (see Supporting Information Scheme S16). In this context, the electrochemical behaviors of all molecular systems have been investigated by CV in ACN. As shown in Figure 4, all compounds exhibit similar behavior with a broad irreversible oxidation process at 0.69, 0.66, and 0.78 V for compounds **1**, **2**, and **3**, respectively. More importantly, almost all CV show the appearance of two new systems between −0.73 and −0.97 V on the reverse scan when the first oxidation process is reached reflecting a strong transformation of the molecular systems at this potential. Indeed, these reduction processes did not appear clearly in the case of compound **2** which can be explained by the lack of solubility of this compound in ACN. On the basis of our previous studies, this typical electrochemical behavior evidences the electro-induced opening of the oxazolidine rings under positive electrochemical stimulation.

At the first sight, the observation of only one oxidation wave may suggest that this oxidation is mainly localized on the BOX units. Despite the effective (but small) effect of substituents (H, Me, and F) on the unique oxidation potential, the latter does not correspond to the typical oxidation potential of the corresponding isolated BOX unit. Moreover, the nonreversible oxidation process observed for all three compounds whatever the nature of the substituent in position 5 does not support this hypothesis.

Indeed, the nature of the substituent on BOX is known to affect its electrochemical behavior. As mentioned above, with a bromine or an hydrogen atom in position 5 (like in compound **1**), the BOX-localized oxidation leads to observe its C−C oxidative coupling characterized on the CV by the emergence of a new redox system at lower potential (ca. 0.39 V).[33,41] At the opposite, a methyl group or a fluorine atom promotes the evolution of the generated radical cation toward the opening of the oxazolidine ring or assure its stability.[33] Here, all three compounds exhibit an identical behavior and the variation of the substituent induces only a minor anodic shift of electrochemical potential (for example, 30 mV between compounds **1** and **2**). On the basis of previous results on simple BT BOX dyad,[34,44] the assignment of this nonreversible oxidation process to the central BT moiety shows that the formation of the corresponding radical cation allows the radical delocalization in the vicinity of one BOX unit to induce its opening and produces, after abstraction of an hydrogen to the media, the **OC** form. Nevertheless, this opening should also induce an anodic shift of the oxidation potential of the BT core because of the generation of an electron-withdrawing group. Consecutively, the conversion between **OC** and **OO** forms should occur at higher potential. For some reasons, this potential variation appears surprisingly limited here and only a broadening of the oxidation wave in place of two distinct peaks is observed on the CV. The position of the anodic peak potential is known to be strongly influenced by the chemical kinetic rate constant when a chemical reaction is coupled to an electron transfer.

As a consequence, a kinetic difference between the first and the second BOX opening can also be envisioned to explain the merging of both processes on the CV. To verify this

DOI: 10.1021/acs.jpcc.9b00546
J. Phys. Chem. C 2019, 123, 11823−11832

assumption, electrochemistry experiments were carried out in thin-layer conditions (TLCV). The reduction of the diffusion layer as well as the potential scan rate allowed observing the splitting of the oxidation wave and then demonstrated a little difference of oxidation potential between **CC** and **OC** forms (Figure 5).

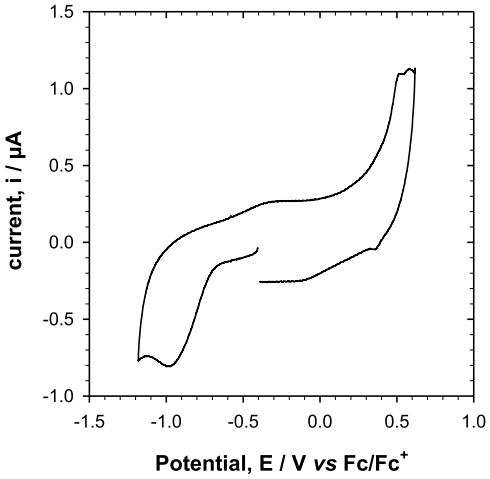

Figure 5. TLCV (<5 μm; 20 mV·s^{-1}) of a solution of **1** in ACN with (TBA)PF_6 (0.1 M) as an electrolyte on a gold electrode.

To confirm the electro-induced opening of both BOX units, spectro-electrochemical experiments have been carried out. As expected, successive coloration/bleaching of the solution of all compounds can be obtained by varying the applied electrochemical potential. As an example, Figure 6 depicts the

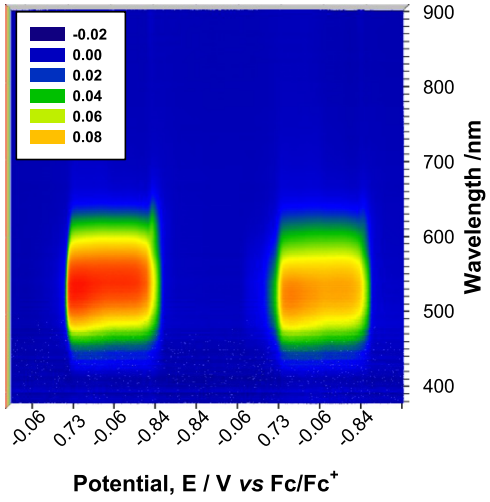

Figure 6. Spectroelectrochemistry in TLCV conditions (~50 μm; 20 mV·s^{-1}) of **1** (0.53 mM) in ACN with (TBA)PF_6 (0.1 M) as an electrolyte on a platinum electrode.

variation of the absorption spectrum of a solution of compound **1** as a function of the applied potential. As soon as the potential reaches 0.69 V, a deep coloration of the solution is observed because of the appearance of an absorption band in the 500−600 nm range. A slight bathochromic shift of the maximum absorption wavelength can be observed during the oxidation process, suggesting two successive processes. Anyway, the perfect overlapping of absorption maxima observed under electrochemical stimulation with these recorded under other kind of stimulations (proton and photon) allows us, assuming that the oxidation of the system leads to the oxazolidine ring opening of both BOX units (from **CC** to **OO** form). By applying −0.9 V, a complete bleaching is observed and the initial state of the solution is restored (**OO** to **CC** form). If the spectro-electrochemical experiments have well confirmed the reversible interconversion between **CC** and **OO** forms, the stepwise commutation of the system was not clearly highlighted certainly because of the tiny difference of oxidation potential between **CC** and **OC** forms (vide supra).

To clarify this point, the commutation of the system was investigated by using an oxidizing reagent such as $NOSbF_6$ (0.87 V vs Fc/Fc^+)[45] which is largely used to evidence mixed valence in electroactive species by UV−visible−NIR spectroscopy[46,47] or generating one-electron oxidation of organic donors.[48] As expected, a drastic change of the UV−visible spectra upon the addition of $NOSbF_6$ aliquots is observed. At the end, we can notice that this addition of oxidizing reagent leads to an identical spectrum as the one obtained after stimulation with an excess of acid as shown in Figure 7 for compound **1**. In addition, initial spectrum can be recovered after treatment with an excess of base such as triethylamine, demonstrating the multimodal switching ability of theses

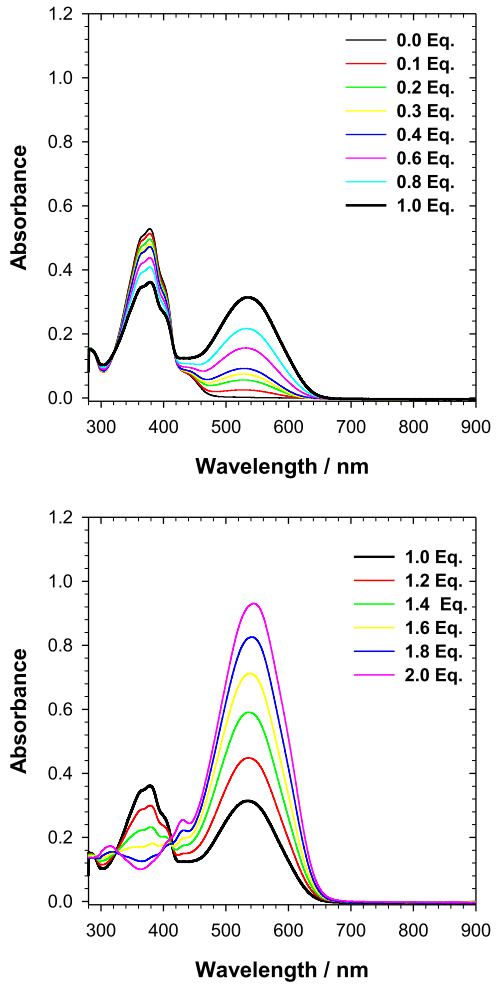

Figure 7. UV−visible spectrum changes of a solution of **BOX-H** in ACN (0.086 mM) upon addition of $NOSbF_6$.

DOI: 10.1021/acs.jpcc.9b00546
J. Phys. Chem. C 2019, 123, 11823−11832

molecular systems. If the UV−visible spectra obtained upon gradual chemical oxidation of compounds (Figure 7, compound **1**) present strong similarities with those chemically and optically induced, subtle differences appear.

Upon addition of 1 equiv of $NOSbF_6$, a unique band centered at 529 nm assigned to the **OC** form (vide infra) appears, being associated with the concomitant decrease of the **CC** characteristic band at 378 nm. The addition of 2 equiv of oxidant leads to the disappearance of the characteristic band of **OC** toward a bathochromically shifted new band (546 nm assigned to **OO** form) and two weak bands at high energy around 300 and 430 nm. Despite these strong similarities, a clear isosbestic point is observed from the beginning of the oxidant addition up to the last addition what could be a clue indicating selective successive processes.

As mentioned above, the ^{19}F NMR spectroscopy not only represents an easy and convenient manner to confirm the stepwise commutation of the system but also probes the selectivity of the addressability under chemical oxidation. The results of the titration of compound **3** by $NOSbF_6$ are presented in Figure 8. The addition of the oxidizing reagent

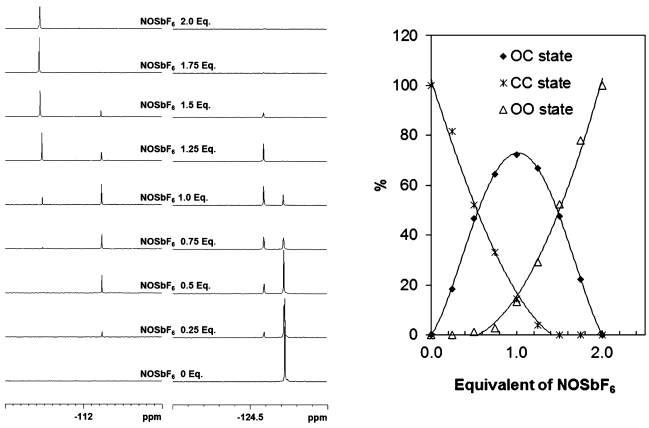

Figure 8. ^{19}F NMR spectrum changes (left) and deduced quantification (right) of the 3 different states of a solution of **BOX-F** in ACN (2.27 mM) upon addition of $NOSbF_6$ aliquots.

induces the appearance of two new peaks (at −124.60 and −112.22 ppm) assigned to the **OC** form. Concerning the **OO** form characterized by a unique peak at −111.49 ppm, its formation starts to be observed after 0.6 equiv but it is somehow very limited. Interestingly, the large formation of **OO** form by chemical oxidation did not lead to its precipitation in ACN as previously observed with acid. This can be easily explained by the change of **OO** counterion nature from a simple chloride to a hexafluoro antimonate anion which is considered as a weakly coordinating anion and should lead generally to more lipophilic salt as generally reported for ionic liquid.[49,50] By measuring the peak intensities, the relative proportion of the three different states of compound **3** as a function of the added amount of oxidizing reagent is plotted (Figure 8). Surprisingly, the ratio between the three species is strongly affected by the nature of the stimulation. As example, **OC** is the predominant form as soon as the amount of $NOSbF_6$ exceeds 0.5 equiv, whereas 0.8 equiv was required with a stimulation by the acid. More generally, we can notice that the **CC** and **OC** forms are totally converted by an electrochemical stimulation after 1 and 2 equiv, respectively, whereas they are still persistent with acid in the same conditions. As consequence, the narrowed coexistence region between the **CC**, **OC**, and **OO** species highlights the higher selectivity and efficiency of the redox addressability compared with other stimuli. Noteworthy, the full conversion from **CC** to **OC** cannot be reached even through the oxidation process. Indeed, the addition of 1 equiv of $NOSbF_6$ led only to the generation of 72% of the **OC** form, which is completed by almost an identical quantity of **OO** and **CC** forms (13 and 15%, respectively). Beside an unselective oxidation of **CC** and **OC**, this behavior can also be explained by considering a possible disproportionation reaction of **OC**. On the basis of the Nernst law, the equilibrium constant of the reaction is directly correlated with the oxidation potential difference (ΔE) between **OC** and **CC** by the following relation 1

$$\Delta E = (E^0_{(CC/OC)} - E^0_{(OC/OO)}) = \frac{RT}{nF} \ln\left(\frac{[CC][OO]}{[OC]^2}\right) = \frac{0.059}{n} \log\ K \quad (1)$$

With R the molar gas constant, T the temperature, F the Faraday constant, and n the number of electron transferred in each redox process. In our case, the observation of only one broad oxidation wave in CV and the slight splitting when TLCV are used are in full agreement with the small oxidation potential difference (0.08 V) calculated by relation 1. To resume, the addition of 1 and 2 equiv of chemical oxidant to **CC** allows its full and selective conversion to **OC** and **OO** form, respectively. However, the **OC** species seems to undergo a disproportionation reaction because of a poor ΔE between **CC** and **OC**. If this latter should be confirmed by further investigation, it avoids the obtainment of pure **OC** but allows its observation with only a mixture with minor quantities of the two other forms.

CONCLUSIONS

In summary, we have elaborated three multimodal molecular switches by the functionalization of a BT unit used as a simple π-conjugated system between two identical BOX moieties. As expected, all three systems exhibit multimodal switching ability under acid, photo-, and electrochemical stimulation. If the opening of both oxazolidine rings can be obtained whatever the nature of the stimulation, we have demonstrated here that a stepwise opening selectivity between two identical BOX units grafted on a BT core can be reached. In all cases, the selectivity between the first and the second opening of both identical BOX units is induced by the variation of the donor character of the whole system, the successive commutation generating a strong electron-withdrawing group. Nevertheless, if this never reported selectivity upon a unique stimulus with two identical switchable units is observed whatever the stimulation, it must be pointed out that its quality depends on the latter.

The direct stimulation of the BOX by acid led to a large coexistence of the three different states of the systems (**OO**, **OC**, and **CC**) over a large range. At the opposite, the indirect stimulation of the BOX via an electromediated process thanks to the electroactivity of the BT allows to enhance the selective addressability between both identical BOX units. This enhancement lays on the evolution of the oxidation potential of the system as a function of the number of commutated BOX. Nevertheless, the poor difference of oxidation potential between **CC** and **OC** forms led to the involvement of **OC** in a

DOI: 10.1021/acs.jpcc.9b00546
J. Phys. Chem. C 2019, 123, 11823−11832

disproportionation reaction avoiding its quantitative conversion.

Nevertheless, these pretty simple systems prepared by an easy condensation are able to modulate a molecular property over three discrete levels. Considered as a proof of concept, they pave the way to more complicated ones where: (i) the addressability efficiency of BOX units through an electro-mediated stimulation can be enhanced by using more complicated linker which is able to exhibit higher ΔE and (ii) more than two BOX units can be connected allowing to improve the number of metastable states which are prime of interest to who is interested in high-density optical memory or multinary logic devices.

■ ASSOCIATED CONTENT

Supporting Information

The Supporting Information is available free of charge on the ACS Publications website at DOI: 10.1021/acs.jpcc.9b00546.

^{1}H NMR spectra of the three different forms (**CC**, **OC**, and **OO**) of all compounds (PDF)

■ AUTHOR INFORMATION

Corresponding Author

*E-mail: lionel.sanguinet@univ-angers.fr.

ORCID

Clément Guerrin: 0000-0002-9216-5130

Stéphanie Delbaere: 0000-0001-6846-6614

Lionel Sanguinet: 0000-0002-4334-9937

Notes

The authors declare no competing financial interest.

■ ACKNOWLEDGMENTS

Y.A. thanks the University of Angers for granting. All authors thank the CARMA and ASTRAL platforms of the Structure Fédérative de Recherche MATRIX, and especially B. Siegler and Dr I. Freuze for their assistance in NMR spectroscopy and MS, respectively.

■ REFERENCES

(1) Pham, H. H.; Gourevich, I.; Jonkman, J. E. N.; Kumacheva, E. Polymer nanostructured material for the recording of biometric features. *J. Mater. Chem.* **2007**, *17*, 523−526.

(2) Zijlstra, P.; Chon, J. W. M.; Gu, M. Five-dimensional optical recording mediated by surface plasmons in gold nanorods. *Nature* **2009**, *459*, 410−413.

(3) Pham, H. H.; Gourevich, I.; Oh, J. K.; Jonkman, J. E. N.; Kumacheva, E. A multidye nanostructured material for optical data storage and security data encryption. *Adv. Mater.* **2004**, *16*, 516−520.

(4) Andréasson, J.; Pischel, U. Smart molecules at work-mimicking advanced logic operations. *Chem. Soc. Rev.* **2010**, *39*, 174−188.

(5) Gust, D.; Andréasson, J.; Pischel, U.; Moore, T. A.; Moore, A. L. Data and signal processing using photochromic molecules. *Chem. Commun.* **2012**, *48*, 1947−1957.

(6) Sun, Z.; Huang, Q.; He, T.; Li, Z.; Zhang, Y.; Yi, L. Multistimuli-responsive supramolecular gels: Design rationale, recent advances, and perspectives. *ChemPhysChem* **2014**, *15*, 2421−2430.

(7) Andréasson, J.; Pischel, U. Molecules with a sense of logic: A progress report. *Chem. Soc. Rev.* **2015**, *44*, 1053−1069.

(8) Andréasson, J.; Pischel, U. Smart molecules at work-mimicking advanced logic operations. *Chem. Soc. Rev.* **2010**, *39*, 174−188.

(9) Andréasson, J.; Pischel, U. Storage and processing of information using molecules: The all-photonic approach with simple and multi-photochromic switches. *Isr. J. Chem.* **2013**, *53*, 236−246.

(10) Irie, M.; Fukaminato, T.; Matsuda, K.; Kobatake, S. Photochromism of diarylethene molecules and crystals: Memories, switches, and actuators. *Chem. Rev.* **2014**, *114*, 12174−12277.

(11) de Silva, A. P.; Vance, T. P.; Wannalerse, B.; West, M. E. S. Molecular logic systems. *Molecular Switches*; Wiley-VCH Verlag GmbH & Co. KGaA, 2011; pp 669−696.

(12) Minkin, V. I. Photoswitchable molecular systems based on spiropyrans and spirooxazines. *Molecular Switches*; Wiley-VCH Verlag GmbH & Co. KGaA, 2011; pp 37−80.

(13) Oms, O.; Hakouk, K.; Dessapt, R.; Deniard, P.; Jobic, S.; Dolbecq, A.; Palacin, T.; Nadjo, L.; Keita, B.; Marrot, J.; Mialane, P. Photo- and electrochromic properties of covalently connected symmetrical and unsymmetrical spiropyran-polyoxometalate dyads. *Chem. Commun.* **2012**, *48*, 12103−12105.

(14) Browne, W. R.; Pollard, M. M.; de lange, B.; Meetsma, A.; Feringa, B. L. Reversible Three-State Switching of Luminescence: A New Twist to Electro- and Photochromic Behavior. *J. Am. Chem. Soc.* **2006**, *128*, 12412−12413.

(15) Ivashenko, O.; Logtenberg, H.; Areephong, J.; Coleman, A. C.; Wesenhagen, P. V.; Geertsema, E. M.; Heureux, N.; Feringa, B. L.; Rudolf, P.; Browne, W. R. Remarkable stability of high energy conformers in self-assembled monolayers of a bistable electro- and photoswitchable overcrowded alkene. *J. Phys. Chem. C* **2011**, *115*, 22965−22975.

(16) Szalóki, G.; Pozzo, J.-L. Synthesis of symmetrical and nonsymmetrical bisthienylcyclopentenes. *Chem.—Eur. J.* **2013**, *19*, 11124−11132.

(17) Fukaminato, T. Single-molecule fluorescence photoswitching: Design and synthesis of photoswitchable fluorescent molecules. *J. Photochem. Photobiol., C* **2011**, *12*, 177−208.

(18) Bertarelli, C.; Bianco, A.; Castagna, R.; Pariani, G. Photochromism into optics: Opportunities to develop light-triggered optical elements. *J. Photochem. Photobiol., C* **2011**, *12*, 106−125.

(19) Tsujioka, T.; Irie, M. Electrical functions of photochromic molecules. *J. Photochem. Photobiol., C* **2010**, *11*, 1−14.

(20) Irie, M. Photochromism of diarylethene single molecules and single crystals. *Photochem. Photobiol. Sci.* **2010**, *9*, 1535−1542.

(21) Irie, M. Photochromism of diarylethene molecules and crystals. *Proc. Jpn. Acad., Ser. B* **2010**, *86*, 472−483.

(22) Yun, C.; You, J.; Kim, J.; Huh, J.; Kim, E. Photochromic fluorescence switching from diarylethenes and its applications. *J. Photochem. Photobiol., C* **2009**, *10*, 111−129.

(23) Wigglesworth, T. J.; Myles, A. J.; Branda, N. R. High-content photochromic polymers based on dithienylethenes. *Eur. J. Org. Chem.* **2005**, 1233−1238.

(24) Tian, H.; Yang, S. Recent progresses on diarylethene based photochromic switches. *Chem. Soc. Rev.* **2004**, *33*, 85−97.

(25) Matsuda, K.; Irie, M. Diarylethene as a photoswitching unit. *J. Photochem. Photobiol., C* **2004**, *5*, 169−182.

(26) Irie, M.; Uchida, K. Synthesis and properties of photochromic diarylethenes with heterocyclic aryl groups. *Bull. Chem. Soc. Jpn.* **1998**, *71*, 985−996.

(27) Harvey, E. C.; Feringa, B. L.; Vos, J. G.; Browne, W. R.; Pryce, M. T. Transition metal functionalized photo- and redox-switchable diarylethene based molecular switches. *Coord. Chem. Rev.* **2015**, *282*−*283*, 77−86.

(28) Jacquemin, D.; Perpète, E. A.; Maurel, F.; Perrier, A. Td-dft simulations of the electronic properties of star-shaped photochromes. *Phys. Chem. Chem. Phys.* **2010**, *12*, 7994−8000.

(29) Sertova, N.; Nunzi, J.-M.; Petkov, I.; Deligeorgiev, T. Photochromism of styryl cyanine dyes in solution. *J. Photochem. Photobiol., A* **1998**, *112*, 187−190.

(30) Bartnik, R.; Lesniak, S.; Mloston, G.; Zielinski, T.; Gebicki, K. Cationic dye derivatives of 1-(2-hydroxyethyl)-2-styryl-3,3-dimethyl-3h-indole. *Chem. Stosow.* **1990**, *34*, 325−334.

(31) Bartnik, R.; Mloston, G.; Cebulska, Z. Synthesis and chain-ring tautomerism of 1-(2-hydroxyethyl)-3,3-dimethyl-3h-indole derivative cyanine dyes. *Chem. Stosow.* **1990**, *34*, 343−352.

(32) Szalóki, G.; Sanguinet, L. Properties and applications of indolinooxazolidines as photo-, electro-, and acidochromic units. In *Photon-working switches*; Yokoyama, Y., Nakatani, K., Eds.; Springer Japan: Tokyo, 2017; pp 69−91.
(33) Hadji, R.; Szalóki, G.; Alévêque, O.; Levillain, E.; Sanguinet, L. The stepwise oxidation of indolino[2,1-b]oxazolidine derivatives. *J. Electroanal. Chem.* **2015**, *749*, 1−9.
(34) Szalóki, G.; Alévêque, O.; Pozzo, J.-L.; Hadji, R.; Levillain, E.; Sanguinet, L. Indolinooxazolidine: A versatile switchable unit. *J. Phys. Chem. B* **2015**, *119*, 307−315.
(35) Blanchard, P.; Cravino, A.; Levillain, E. Electrochemistry of oligothiophenes and polythiophenes. In *Handbook of Thiophene-Based Materials*; John Wiley & Sons, Ltd., 2009; pp 419−453.
(36) Bader, M. M.; Pham, P.-T. T.; Elandaloussi, E. H. Dicyanovinyl-substituted oligothiophenes. *Cryst. Growth Des.* **2010**, *10*, 5027−5030.
(37) Szalóki, G.; Sanguinet, L. Silica-mediated synthesis of indolinooxazolidine-based molecular switches. *J. Org. Chem.* **2015**, *80*, 3949−3956.
(38) Sevez, G.; Gan, J.; Delbaere, S.; Vermeersch, G.; Sanguinet, L.; Levillain, E.; Pozzo, J.-L. Photochromic performance of a dithienylethene-indolinooxazolidine hybrid. *Photochem. Photobiol. Sci.* **2010**, *9*, 131−135.
(39) Alévêque, O.; Levillain, E.; Sanguinet, L. Spectroelectrochemistry on electroactive self-assembled monolayers: Cyclic voltammetry coupled to spectrophotometry. *Electrochem. Commun.* **2015**, *51*, 108−112.
(40) Abu-Eittah, R. H.; Al-Sugeir, F. A. Studies on the Electronic Absorption Spectra of 2,2′-Bithienyl and Some of Its Derivatives. A Molecular Orbital Treatment. *Bull. Chem. Soc. Jpn.* **1985**, *58*, 2126−2132.
(41) Sanguinet, L.; Berthet, J.; Szalóki, G.; Alévêque, O.; Pozzo, J.-L.; Delbaere, S. 13 metastable states arising from a simple multifunctional unimolecular system. *Dyes Pigments* **2017**, *137*, 490−498.
(42) Guerrin, C.; Szalóki, G.; Berthet, J.; Sanguinet, L.; Orio, M.; Delbaere, S. Indolino-oxazolidine acido- and photochromic system investigated by nmr and density functional theory calculations. *J. Org. Chem.* **2018**, *83*, 10409−10419.
(43) Chen, Q.; Sheng, L.; Du, J.; Xi, G.; Zhang, S. X.-A. Photooxidation of oxazolidine molecular switches: Uncovering an intramolecular ionization facilitated cyclization process. *Chem. Commun.* **2018**, *54*, 5094−5097.
(44) Bondu, F.; Hadji, R.; Szalóki, G.; Alévêque, O.; Sanguinet, L.; Pozzo, J.-L.; Cavagnat, D.; Buffeteau, T.; Rodriguez, V. Huge electro-/photo-/acidoinduced second-order nonlinear contrasts from multi-addressable indolinooxazolodine. *J. Phys. Chem. B* **2015**, *119*, 6758−6765.
(45) Kochi, J. K. Inner-sphere electron transfer in organic chemistry. Relevance to electrophilic aromatic nitration. *Acc. Chem. Res.* **1992**, *25*, 39−47.
(46) Cotelle, Y.; Hardouin-Lerouge, M.; Legoupy, S.; Alévêque, O.; Levillain, E.; Hudhomme, P. Glycoluril-tetrathiafulvalene molecular clips: on the influence of electronic and spatial properties for binding neutral accepting guests. *Beilstein J. Org. Chem.* **2015**, *11*, 1023−1036.
(47) Ran, Y.-F.; Blum, C.; Liu, S.-X.; Sanguinet, L.; Levillain, E.; Decurtins, S. A tetrathiafulvalene-functionalized schiff base macrocycle: Synthesis, electrochemical, and photophysical properties. *Tetrahedron* **2011**, *67*, 1623−1627.
(48) Sasamori, T.; Tokitoh, N.; Streubel, R. Π-electron redox systems of heavier group 15 elements. In *Organic Redox Systems*; Nishinaga, T., Ed.; John Wiley & Sons, 2015.
(49) Olivier-Bourbigou, H.; Magna, L. Ionic liquids: Perspectives for organic and catalytic reactions. *J. Mol. Catal. A: Chem.* **2002**, *182*−*183*, 419−437.
(50) Longo, L. S.; Smith, E. F.; Licence, P. Study of the stability of 1-alkyl-3-methylimidazolium hexafluoroantimonate(v) based ionic liquids using x-ray photoelectron spectroscopy. *ACS Sustainable Chem. Eng.* **2016**, *4*, 5953−5962.

DOI: 10.1021/acs.jpcc.9b00546
J. Phys. Chem. C 2019, 123, 11823−11832